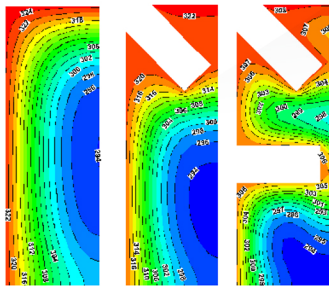
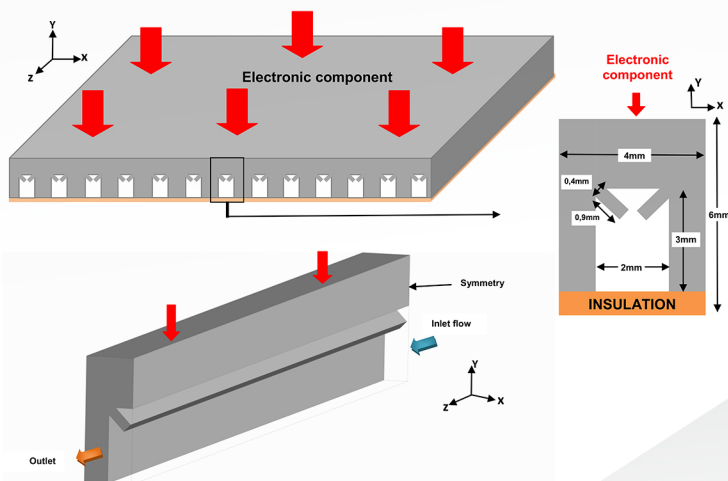


Mechanical Engineering Technologies and Applications



Editor:
Zied Driss

Bentham Books

Mechanical Engineering Technologies and Applications

(Volume 3)

Edited by

Zied Driss

Laboratory of Electromechanical Systems (LASEM)

National School of Engineers of Sfax (ENIS)

University of Sfax (US)

Sfax, Tunisia

Mechanical Engineering Technologies and Applications

(Volume 3)

Editor: Zied Driss

ISSN (Online): 2811-0455

ISSN (Print): 2811-0463

ISBN (Online): 978-981-5179-27-9

ISBN (Print): 978-981-5179-28-6

ISBN (Paperback): 978-981-5179-29-3

© 2023, Bentham Books imprint.

Published by Bentham Science Publishers Pte. Ltd. Singapore. All Rights Reserved.

First published in 2023.

BENTHAM SCIENCE PUBLISHERS LTD.

End User License Agreement (for non-institutional, personal use)

This is an agreement between you and Bentham Science Publishers Ltd. Please read this License Agreement carefully before using the ebook/echapter/ejournal (“**Work**”). Your use of the Work constitutes your agreement to the terms and conditions set forth in this License Agreement. If you do not agree to these terms and conditions then you should not use the Work.

Bentham Science Publishers agrees to grant you a non-exclusive, non-transferable limited license to use the Work subject to and in accordance with the following terms and conditions. This License Agreement is for non-library, personal use only. For a library / institutional / multi user license in respect of the Work, please contact: permission@benthamscience.net.

Usage Rules:

1. All rights reserved: The Work is the subject of copyright and Bentham Science Publishers either owns the Work (and the copyright in it) or is licensed to distribute the Work. You shall not copy, reproduce, modify, remove, delete, augment, add to, publish, transmit, sell, resell, create derivative works from, or in any way exploit the Work or make the Work available for others to do any of the same, in any form or by any means, in whole or in part, in each case without the prior written permission of Bentham Science Publishers, unless stated otherwise in this License Agreement.
2. You may download a copy of the Work on one occasion to one personal computer (including tablet, laptop, desktop, or other such devices). You may make one back-up copy of the Work to avoid losing it.
3. The unauthorised use or distribution of copyrighted or other proprietary content is illegal and could subject you to liability for substantial money damages. You will be liable for any damage resulting from your misuse of the Work or any violation of this License Agreement, including any infringement by you of copyrights or proprietary rights.

Disclaimer:

Bentham Science Publishers does not guarantee that the information in the Work is error-free, or warrant that it will meet your requirements or that access to the Work will be uninterrupted or error-free. The Work is provided "as is" without warranty of any kind, either express or implied or statutory, including, without limitation, implied warranties of merchantability and fitness for a particular purpose. The entire risk as to the results and performance of the Work is assumed by you. No responsibility is assumed by Bentham Science Publishers, its staff, editors and/or authors for any injury and/or damage to persons or property as a matter of products liability, negligence or otherwise, or from any use or operation of any methods, products instruction, advertisements or ideas contained in the Work.

Limitation of Liability:

In no event will Bentham Science Publishers, its staff, editors and/or authors, be liable for any damages, including, without limitation, special, incidental and/or consequential damages and/or damages for lost data and/or profits arising out of (whether directly or indirectly) the use or inability to use the Work. The entire liability of Bentham Science Publishers shall be limited to the amount actually paid by you for the Work.

General:

1. Any dispute or claim arising out of or in connection with this License Agreement or the Work (including non-contractual disputes or claims) will be governed by and construed in accordance with the laws of Singapore. Each party agrees that the courts of the state of Singapore shall have exclusive jurisdiction to settle any dispute or claim arising out of or in connection with this License Agreement or the Work (including non-contractual disputes or claims).
2. Your rights under this License Agreement will automatically terminate without notice and without the

need for a court order if at any point you breach any terms of this License Agreement. In no event will any delay or failure by Bentham Science Publishers in enforcing your compliance with this License Agreement constitute a waiver of any of its rights.

3. You acknowledge that you have read this License Agreement, and agree to be bound by its terms and conditions. To the extent that any other terms and conditions presented on any website of Bentham Science Publishers conflict with, or are inconsistent with, the terms and conditions set out in this License Agreement, you acknowledge that the terms and conditions set out in this License Agreement shall prevail.

Bentham Science Publishers Pte. Ltd.

80 Robinson Road #02-00

Singapore 068898

Singapore

Email: subscriptions@benthamscience.net



CONTENTS

PREFACE	i
LIST OF CONTRIBUTORS	iii
CHAPTER 1 THREE-DIMENSIONAL MIXED CONVECTION IN A CUBICAL CAVITY WITH NANOFLUID	1
<i>Bellout Saliha and Bessaïh Rachid</i>	
INTRODUCTION	1
MATHEMATICAL FORMULATION	2
Problem Description	2
Numerical Method and Code Validation	5
RESULTS AND DISCUSSION	6
Reynolds Effect	6
Volume Fraction Effect	9
Heat Source Location Effect	11
CONCLUSION	12
REFERENCES	13
CHAPTER 2 AN ELEMENT-FREE GALERKIN ANALYSIS OF HYPERELASTIC MATERIALS	15
<i>El Hassan Boudaia, Lahbib Bousshine and Abdelmajid Daya</i>	
INTRODUCTION	15
GOVERNING EQUATIONS	16
MOVING LEAST SQUARES APPROXIMATION	19
THE EFGM FORMULATION OF HYPERELASTICITY	21
NUMERICAL RESULT	22
CONCLUSION	24
REFERENCES	25
CHAPTER 3 3D NUMERICAL MODELING OF FLOWS ON A PHYSICAL MODEL OF A SKI-JUMP SPILLWAY	26
<i>Seddik Shiri</i>	
INTRODUCTION	26
BASIC THEORY OF THE SPH METHOD	28
NUMERICAL MODELING	29
Presentation of the Model	29
Materials Modelling	31
SPH Particles Generation and FE Mesh	32
Boundary Conditions and Interactions	32
RESULTS AND DISCUSSION	32
CONCLUSION	41
ACKNOWLEDGEMENT	42
REFERENCES	42
CHAPTER 4 TURBINE SWIRLING DEVICE EFFECT ON LPG-H2 ENGINE IN-CYLINDER FLOW MOTION AT INTAKE STROKE	44
<i>Sahar Hadjkacem, Mohamed Ali Jemni, Zied Driss and Mohamed Salah Abid</i>	
INTRODUCTION	44
NUMERICAL APPROACH	46
GEOMETRICAL MODEL	46
BOUNDARIES AND INITIAL CONDITIONS	46
NUMERICAL RESULTS AND DISCUSSION	47

In-cylinder Flow Velocity	48
In-Cylinder Swirl Motion	49
Turbulent Kinetic Energy	49
CONCLUSION	50
APPENDIX	50
ACKNOWLEDGEMENT	51
REFERENCES	51
CHAPTER 5 ARTIFICIAL NEURAL NETWORKS APPROACH FOR CROSS-FLOW HEAT EXCHANGER FOULING MODELING	54
<i>Rania Jradi, Christophe Marvillet and Mohamed Razak Jeday</i>	
INTRODUCTION	54
ARTIFICIAL NEURAL NETWORK STRUCTURE AND METHODOLOGY	56
ARTIFICIAL NEURAL NETWORK MODEL	59
CONCLUSION	61
REFERENCES	61
CHAPTER 6 THE EFFECT OF THE NITROGEN PERCENTAGE ON THE MICROSTRUCTURE AND MECHANICAL PROPERTIES OF ZR-N COATINGS	63
<i>Linda Aissani, Nourredine Belghar and Zied Driss</i>	
INTRODUCTION	63
Experimental Detail	65
RESULTS AND DISCUSSION	67
Chemical Composition	67
Crystalline Structure	67
Morphology	68
Mechanical Property	70
CONCLUSION	70
REFERENCES	71
CHAPTER 7 NON-NEWTONIAN PSEUDOPLASTIC FLUID FLOW AND HEAT TRANSFER INSIDE A HORIZONTAL DUCT: NEW CORRELATIONS	72
<i>Horimek Abderrahmane, Abed Saad and Ait-Messaoudene Nouredine</i>	
INTRODUCTION	72
FORMULATION OF THE PROBLEM	75
RESULTS AND DISCUSSION	80
CONCLUSION	86
REFERENCES	87
CHAPTER 8 DESIGN, MATHEMATICAL MODELING AND THERMAL PERFORMANCE EVALUATION OF WATER SOLAR COLLECTOR FOR THE DESALINATION PROCESS	89
<i>K. Zarzoum, K. Zhani and H. Ben Bacha</i>	
INTRODUCTION	89
MATERIALS AND METHODS	92
Collector Design and Equipment	92
Dynamic Modeling Approach	93
Models Approximation of the Solar Collector	97
Experimental Study of the Water Solar Collector	97
Numerical Simulation of Water Solar Collector	101
Numerical Simulation in Dynamic Regime of an Air Solar Heater	101
CONCLUSION	103
ACKNOWLEDGEMENTS	104
REFERENCES	104

CHAPTER 9 STRUCTURAL AND MECHANICAL PROPERTIES OF TI-N FILMS –	
ABINITIO CALCULATIONS AND EXPERIMENT	106
<i>Sara Fares, Linda Aissani, Abdehak Ayad, Noureddine Belghar and Zied Driss</i>	
INTRODUCTION	107
COMPUTATIONAL DETAILS	108
Experimental Detail	109
RESULTS AND DISCUSSION	110
Structural Properties	110
CONCLUSION	114
ACKNOWLEDGEMENTS	115
REFERENCES	115
SUBJECT INDEX	118

PREFACE

This book focuses on the dissemination of information of permanent interest in mechanic applications and engineering technology. The considered applications are widely used in several industrial fields particularly in those of automotive and aerospace aspects. Many features related to Mechanic processes are presented. The presented case studies and development approaches aim to provide the readers, such as engineers and PhD students, with basic and applied studies broadly related to the Mechanic Applications and Engineering Technology.

The first chapter reports numerical simulations of three-dimensional laminar mixed convection heat transfer of water-based- Al_2O_3 nanofluid in an open cubic cavity with a heated block. Ansys-Fluent was used to simulate 3D flows with heat transfer.

In the second chapter, nonlinear formulations of the Element-Free Galerkin Method (EFGM) are presented for the large deformation analysis of Ogden's hyperelastic materials, which are considered incompressible. The EFGM requires no explicit mesh in computation and therefore avoids mesh distortion difficulties.

In the third chapter, a 3D numerical modeling with the LS-DYNA commercial code was developed using a coupled SPH-FEM method (Smoothed Particle Hydrodynamics (SPH) and Finite element method (FEM)) to simulate the hydraulic behavior of a physical model Ski-Jump Spillway with dentates. Several examples of validation, taken from the literature, demonstrate the precision and reliability of developed numerical models.

The fourth chapter focuses on improving the inlet system of an LPG-H₂ fueled engine by adding a static inclined blade turbine. It is a horizontal rotational axis turbine with four blades evenly distributed with an angle of inclination of 35°. Computational Fluid Dynamics (CFD) simulations are used in order to capture the in-cylinder flow motion and its influence on the flow characteristics. The method is assessed by application to flow calculations in the intake manifold for 3000 rpm engine speed.

The purpose of the fifth chapter is to explain the effective utilization of the Artificial Neural Networks (ANN) model in heat transfer applications for thermal problems, like fouling in a heat exchanger. The application of the ANN tool with different techniques and structures shows that it is an effective and powerful tool due to its small errors in comparison with experimental data.

The sixth chapter investigates the effect of nitrogen concentration, as a reactive gas, on the structure and properties of ZrN coatings deposited by magnetron sputtering. The structural and morphological properties of Zr-N films were described, followed by a detailed investigation of the mechanical properties of Zr-N coatings. By varying the nitrogen percentage, the structure and the hardness of Zr-N films were evaluated in a wide range.

In the seventh chapter, the problem of forced convection in a simple horizontal cylindrical pipe is studied. Two boundary conditions are considered, uniform constant heat flux and uniform temperature. The fluid to be heated is pseudoplastic, modeled by the Ostwald law ($n \leq 1.0$). A fully developed velocity profile is assumed at the pipe entrance. The energy equation is solved numerically with a simple implicit finite difference scheme.

ii

The eighth chapter presents the modeling and the experimental study of a water solar collector coupled to an optimized solar still developed in order to boost freshwater production in a solar distillation system. The desalination process is currently operated under the climatological conditions of Sfax, Tunisia. To numerically simulate the water solar collector, a dynamic model based on heat and mass transfer of the water solar collector was developed.

In the ninth chapter, the effect of film thickness on the structure and properties of Ti-N films deposited by magnetron sputtering are investigated. The structural properties of Ti-N films were described, followed by a detailed investigation into their mechanical properties by using theoretical and experimental analysis. The theoretical calculation presented the Rocksalt TiN structure with a lattice parameter of about 4.255 Å are confirmed by X-ray diffraction.

Zied Driss

Laboratory of Electromechanical Systems (LASEM)

National School of Engineers of Sfax (ENIS)

University of Sfax (US)

Sfax, Tunisia

List of Contributors

Abdelmajid Daya	Laboratory of MMESA, Faculty of Science and Technology, Errachidia, Morocco
Abed Saad	Department of Mechanical Engineering, Ziane Achour University, Djelfa, Algeria
Ait-Messaoudene Nouredine	Laboratoire des Applications Energétiques de l'Hydrogène (LApEH), Blida University 1, Blida, Algeria
Abdehak Ayad	Laboratoire Microstructures et Défauts dans les Matériaux, Univeristé Frères Mentouri Constantine 1, Route Ain El Bey, Constantine, Algeria Département de Pharmacie, Faculté de Médecine. Université Salah Boubnider Constantine 3 Nouvelle ville Ali Mendjeli, Constantine, Algeria
Bellout Saliha	LEAP Laboratory, Department of Mechanical Engineering, Faculty of Sciences Technology, University of Brothers Mentouri-Constantine 1, Route de Ain El. Bey, Constantine, Algeria
Bessaïh Rachid	LEAP Laboratory, Department of Mechanical Engineering, Faculty of Sciences Technology, University of Brothers Mentouri-Constantine 1, Route de Ain El. Bey, Constantine, Algeria
Christophe Marvillet	CMGPCE Laboratory, French Institute of Refrigeration (IFFI), National Conservatory of Arts and Crafts of Paris (CNAM), Paris, France
El Hassan Boudaia	Laboratory of Mechanics, Engineering and Innovation, Higher School of Technology, Casablanca, Morocco
Horimek Abderrahmane	Department of Mechanical Engineering, Ziane Achour University, Djelfa, Algeria
H. Ben Bacha	Department of Mechanical Engineering, College of Engineering at Alkharj, Prince Sattam Bin Abdulaziz University, Alkharj, Kingdom of Saudi Arabia
K. Zarzoum	LASEM (Electromechanical Systems Laboratory), National Engineering School of Sfax, Sfax University, Sfax, Tunisia
K. Zhani	Department of Mechanical Engineering, College of Engineering, University of Bisha, Bisha, Kingdom of Saudi Arabia
Lahbib Bousshine	Laboratory of Mechanics, Engineering and Innovation, ENSEM, University of Hassan II, Casablanca, Morocco
Linda Aissani	Department of Mater Science, Abbès Laghrour University of Khenchela, Khenchela, Algeria Laboratory of Active Components and Materials, Larbi Ben M'hidi University of Oum El Bouaghi, Oum El Bouaghi, Algeria
Mohamed Ali Jemni	Laboratory of Electromechanical Systems (LASEM), National School of Engineers of Sfax (ENIS), University of Sfax (US), Sfax, Tunisia
Mohamed Salah Abid	Laboratory of Electromechanical Systems (LASEM), National School of Engineers of Sfax (ENIS), University of Sfax (US), Sfax, Tunisia
Mohamed Razak Jeday	Research Laboratory, Process, Energy, Environment and Electrical Systems, National Engineering School of Gabes (ENIG), University of Gabes, Gabes, Tunisia

iv

Nourredine Belghar	LGEM Laboratory, University of Biskra, Biskra, Algeria
Rania Jradi	Research Laboratory, Process, Energy, Environment and Electrical Systems, National Engineering School of Gabes (ENIG), University of Gabes, Gabes, Tunisia
Seddik Shiri	National Engineering School of Bizerte, University of Carthage, Research Laboratory on Applied Mechanics and Engineering, Tunis, Tunisia
Sahar Hadjkacem	Laboratory of Electromechanical Systems (LASEM), National School of Engineers of Sfax (ENIS), University of Sfax (US), Sfax, Tunisia
Sara Fares	Laboratoire Microstructures et Défauts dans les Matériaux, Univeristé Frères Mentouri Constantine 1, Route Ain El Bey, Constantine, Algeria
Zied Driss	Laboratory of Electromechanical Systems (LASEM), National School of Engineers of Sfax (ENIS), University of Sfax (US), Sfax, Tunisia

CHAPTER 1

Three-Dimensional Mixed Convection in a Cubical Cavity with Nanofluid**Bellout Saliha^{1,*} and Bessaïh Rachid¹**¹ *LEAP Laboratory, Department of Mechanical Engineering, Faculty of Sciences Technology, University of Brothers Mentouri-Constantine 1, Route de Ain El. Bey, Constantine, Algeria*

Abstract: The present study reports numerical simulations of three-dimensional laminar mixed convection heat transfer of water-based- Al_2O_3 nanofluid in an open cubic cavity with a heated block. Ansys-Fluent 14.5 was used to simulate 3D flows with heat transfer. Streamlines, isotherms, vertical velocity profile, and local Nusselt numbers are presented for Reynolds numbers in the range ($300 < \text{Re} < 700$), volume fractions of nanoparticles ($0 < \phi < 0.08$) and heat source location ($1\text{cm} < d < 3\text{cm}$). It was found that when adding nanoparticles to the base fluid or increasing the volume fraction of nanoparticles, the Nusselt number increases. Moreover, the heat transfer rate increases when the Reynolds number increases.

Keywords: Cubical cavity, Heated block, Mixed convection, Nanofluid.

INTRODUCTION

The improvement of heat transfer by mixed convection is the main object of several works. There is a real demand in the industrial world for new strategies allowing improving the thermal behaviour of fluids in the cooling system. This new fluid concept is called “nanofluid”. The idea is then to insert solid particles of nanometric size into liquids to improve the mixture's thermal performance. Their syntheses meet the needs of improving thermal properties and is the most promising solution in heat transfer improvement.

This interest in nanofluids was reflected in numerous technological and industrial applications; since 1995, numerous experimental and numerical studies were carried out on convection with nanofluids [1 - 7].

* **Corresponding author Bellout Saliha:** LEAP Laboratory, Department of Mechanical Engineering, Faculty of Sciences Technology, University of Brothers Mentouri-Constantine 1, Route de Ain El. Bey, Constantine, Algeria; E-mail: belloutsaliha@gmail.com.

The objective of the present study is to numerically simulate the heat transfer properties by mixed convection of a nanofluid (Al_2O_3 -water) in an open cubic cavity, heated by a heat source; the effects of Reynolds number, the volume fraction and the position of the heat source are studied to improve heat exchange.

MATHEMATICAL FORMULATION

Problem Description

The physical model considered is a cubic cavity of $L = 5\text{cm}$, shown schematically in Fig. (1). The volumetric heat source (q_v) is placed on the lower wall of the cavity; the other walls are adiabatic. The nanofluid enters at a speed of U_0 and a temperature T_0 .

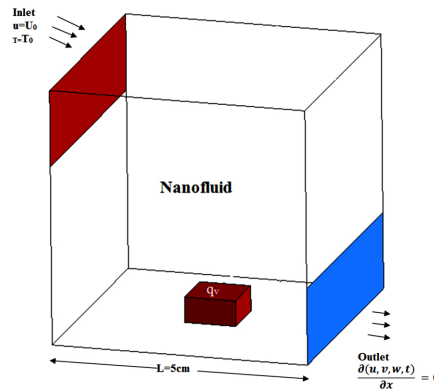


Fig. (1). Cubical cavity filled with nanofluid (Al_2O_3 / Water).

The equations governing the flow and heat transfer are written as follows:

Continuity:

$$\frac{\partial u}{\partial x} + \frac{\partial v}{\partial y} + \frac{\partial w}{\partial z} = 0 \quad (1)$$

x-momentum:

$$u \frac{\partial u}{\partial x} + v \frac{\partial u}{\partial y} + w \frac{\partial u}{\partial z} = \frac{1}{\rho_{nf}} \left[-\frac{\partial p}{\partial x} + \mu_{nf} \left(\frac{\partial^2 u}{\partial x^2} + \frac{\partial^2 u}{\partial y^2} + \frac{\partial^2 u}{\partial z^2} \right) \right] \quad (2)$$

y-momentum:

$$u \frac{\partial v}{\partial x} + v \frac{\partial v}{\partial y} + w \frac{\partial v}{\partial z} = \frac{1}{\rho_{nf}} \left[-\frac{\partial p}{\partial y} + \mu_{nf} \left(\frac{\partial^2 v}{\partial x^2} + \frac{\partial^2 v}{\partial y^2} + \frac{\partial^2 v}{\partial z^2} \right) \right] + (\rho\beta)_{nf} g (T - T_0) \quad (3)$$

z-momentum:

$$u \frac{\partial w}{\partial x} + v \frac{\partial w}{\partial y} + w \frac{\partial w}{\partial z} = \frac{1}{\rho_{nf}} \left[-\frac{\partial p}{\partial z} + \mu_{nf} \left(\frac{\partial^2 w}{\partial x^2} + \frac{\partial^2 w}{\partial y^2} + \frac{\partial^2 w}{\partial z^2} \right) \right] \quad (4)$$

Energy:

In the fluid region:

$$(\rho C_p)_{nf} \left(u \frac{\partial T}{\partial x} + v \frac{\partial T}{\partial y} + w \frac{\partial T}{\partial z} \right) = k_{nf} \left(\frac{\partial^2 T}{\partial x^2} + \frac{\partial^2 T}{\partial y^2} + \frac{\partial^2 T}{\partial z^2} \right) \quad (5a)$$

In the Solid Region (Heat Source):

$$k_{nf} \left(\frac{\partial^2 T}{\partial x^2} + \frac{\partial^2 T}{\partial y^2} + \frac{\partial^2 T}{\partial z^2} \right) + q_v = 0 \quad (5b)$$

The thermophysical properties of the nanofluid are defined as follows [8 - 10]:

$$\rho_{nf} = (1 - \phi) \rho_f + \phi \rho_p \quad (6)$$

$$(\rho C_p)_{nf} = (1 - \phi) (\rho C_p)_f + \phi (\rho C_p)_p \quad (7)$$

CHAPTER 2

An Element-Free Galerkin Analysis of Hyperelastic Materials**El Hassan Boudaia^{1,*}, Lahbib Bousshine² and Abdelmajid Daya³**¹ *Laboratory of Mechanics, Engineering and Innovation, Higher School of Technology, Casablanca, Morocco*² *Laboratory of Mechanics, Engineering and Innovation, ENSEM, University of Hassan II, Casablanca, Morocco*³ *Laboratory of MMESA, Faculty of Science and Technology, Errachidia, Morocco*

Abstract: Nonlinear formulations of the Element-Free Galerkin Method (EFGM) are presented for the large deformation analysis of Ogden's hyperelastic materials, which are considered incompressible. The EFGM requires no explicit mesh in computation and therefore avoids mesh distortion difficulties. In this study, the implementation of the Moving Least Squares (MLS) approximation with the quartic spline weight function is used to obtain the shape function and the transformation method is proposed to impose the essential boundary conditions. Numerical results for a typical example show that the present method is effective in dealing with large deformation hyperelastic materials problems.

Keywords: Element-free galerkin method, Hyperelasticity, Moving least squares, Numerical analysis, Transformation method.

INTRODUCTION

The importance of large deformation problems in the manufacture of rubber products is increasing. Thus far, these deformations can be analyzed by the finite element method (FEM). However, large deformation causes severe mesh distortions in elements near the boundary, thereby reducing the stable time increment while obtaining the solution. On the other hand, particle methods are meshless techniques that no longer use connectivity data.

Therefore, users do not encounter such problems where the use of the element-free Galerkin method (EFGM) requires no explicit mesh in computation and therefore avoids mesh distortion difficulties.

* **Corresponding author to El Hassan Boudaia:** Laboratory of Mechanics, Engineering and Innovation, Higher School of Technology, Casablanca, Morocco; E-mail: boudelhassan@yahoo.fr

In the last decade, Belytschko *et al.* [1], introduced the EFGM based on the diffuse elements method (DEM) originated by Nayroles *et al.* [2]. Currently, several monographs on Meshless or Meshfree methods have been published. Among these, we mention the famous book of Liu [3], who provided a systematic discussion on basic theories, and fundamentals for Meshfree methods, especially on Meshfree weak-form methods. It provides a comprehensive record of well-known Meshfree methods and the wide coverage of applications of Meshfree methods to problems of elastic solids mechanics (beams, plates, shells, *etc.*) as well as fluid mechanics. On the other hand, the complex variable element-free Galerkin method for elasto-plasticity problems is treated by Peng and Cheng [4], whereas the plasticity of solids is developed by Chen *et al.* [5]. However, the important works of hyperelastic materials were proposed by Bonet and Wood [6].

For the sake of clarity, this paper is divided into two parts: The first part, consisting of three sections, concerns methods and materials. In the first section, the description of large deformations is discussed. On the other hand, the second section is dedicated to the Moving Least Squares (MLS) approximation given by Fasshauer [7] and the transformation method proposed by Boudaia and Bousshine [8] to impose the essential boundary conditions. While the third section deals with the EFGM formulation of hyperelasticity [9]. Then the second part, concerning results and discussion, illustrates in the last section a numerical example of a large strain problem to validate the proposed method. Finally, this paper is closed with a general conclusion.

GOVERNING EQUATIONS

Note \vec{x} and \vec{X} position vectors of a particle P of a deformable body in the current configuration (where the solid occupies the volume Ω) and initial configuration (where the solid occupies the volume Ω_0). We will use the same reference $({}^0, \vec{e}_1, \vec{e}_2, \vec{e}_3)$ for the initial configuration C_0 given at time t_0 and deformed configuration C_t at time t , as shown in Fig. (1).

For a Lagrangian description, the movement of the body can be defined relative to a reference configuration C_0 , by a vector function:

$$\Phi : \begin{cases} C_0 \rightarrow C_t \\ \vec{X} \mapsto \vec{x} = \Phi(\vec{X}, t) \end{cases} \quad (1)$$

By introducing the displacement vector \vec{u} and we write the eq. (1) in the equivalent form:

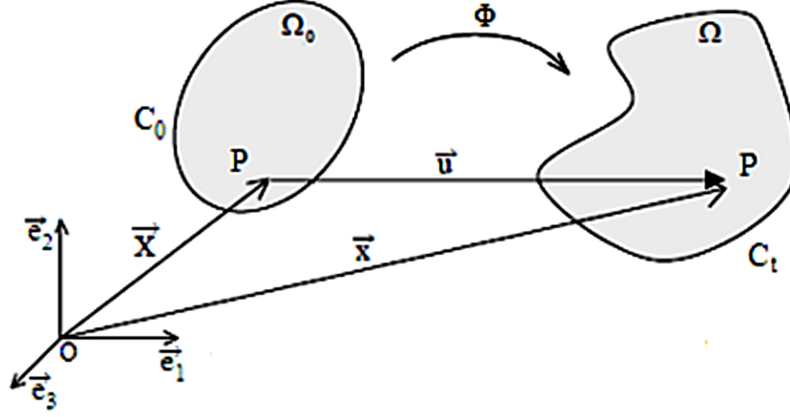


Fig. (1). Initial and deformed configurations.

$$\vec{x} = \vec{X} + \vec{u}(\vec{X}, t) \quad (2)$$

In order to describe the geometric transformations associated with these large strains, we introduce the deformation gradient tensor F defined by:

$$F_{ij}(\vec{X}, t) = \frac{\partial \Phi_i(\vec{X}, t)}{\partial X_j} = \frac{\partial x_i}{\partial X_j} = \delta_{ij} + \frac{\partial u_i}{\partial X_j} \quad (3)$$

where δ_{ij} denotes the Kronecker symbol.

Or eq. (3) can be written in the matrix form:

$$F = I + \nabla u \quad (4)$$

where I is the unit tensor, ∇ is the displacement gradient tensor.

Due to the large displacements and large rotations, the Green–Lagrangian strain tensor E is defined by:

$$E = (C - I) / 2 \quad (5)$$

where $C = F^T F$ is the right Cauchy–Green deformation tensor.

3D Numerical Modeling of Flows on a Physical Model of a Ski-Jump Spillway

Seddik Shiri^{1,*}

¹ National Engineering School of Bizerte, University of Carthage, Research Laboratory on Applied Mechanics and Engineering, Tunis, Tunisia

Abstract: Plunge pools are a very economical means of discharging high energy flows downstream of dams. However, the high energy discharge usually falls down from a considerable height with high velocity, which leads to the phenomenon of erosion due to the detachment and transport of solid particles by hydraulic forces. This pathology which is common in earth structures can lead to their failure, therefore, the understanding and the prediction of this risk are of paramount importance. In this study, a 3D numerical modeling with the LS-DYNA commercial code was developed using a coupled SPH-FEM method (Smoothed Particle Hydrodynamics (SPH) and Finite element method (FEM)) to simulate the hydraulic behavior of a physical model Ski-Jump Spillway with dentates. The water flow in the tunnels and on the ski jumps, as well as the trajectories of the jets and the impact zones could be determined for several study cases. Several examples of validation, taken from the literature, demonstrate the precision and reliability of developed numerical models.

Keywords: Coupled SPH-FEM approach, Hydraulic, Physical model, Spillway, Ski jump, Water flow.

INTRODUCTION

A dam is a structure built to accumulate a large quantity of water that can be intended for multiple uses: irrigation, supply of drinking water, production of hydroelectricity, flood control, nautical activities, *etc.* The spillway is one of the most important related elements of the dam. It allows excess water flows to be evacuated when the reservoir reaches a limit level and to send it downstream.

In recent years, dam safety has attracted more attention from experts and the general public. This is mainly due to the fact that incidents still occur.

* **Corresponding author Seddik Shiri:** National Engineering School of Bizerte, University of Carthage, Research Laboratory on Applied Mechanics and Engineering, Tunis, Tunisia; E-mail: seddik.shiri@enib.ucar.tn

The 2017 Oroville Dam crisis, associated with the risk of collapse of the main spillway of the tallest dam in the United States, is probably the most recent incident.

Hydraulic studies of spillways have long been carried out experimentally through the use of reduced physical models. In recent decades, continuous progress in efficient numerical techniques and the increase in the capacity of large computers have made numerical modeling a powerful tool to complement physical modeling. Numerical hydrodynamic models can provide a number of relevant answers to all the physical phenomena that govern flows in spillways, which can thus limit the number of the necessary experimental campaigns. Numerical modeling of spillways often involves complex geometries and multi-physical phenomena (water jet, pit digging, erosion, *etc.*).

Several numerical methods are used to model the spillways:

- Classical numerical methods are based on meshes such as the finite element method (FEM) and the finite volume method (FVM) [1 - 4, 18].
- Meshfree or non-mesh methods [5 - 9, 17, 19 - 21]. These new methods have appeared over the past few decades to overcome the limitations of the finite element method, such as the extreme distortion of meshes in the event of large deformations.

Physical and numerical modeling tools for ski jump spillways have developed enormously in recent years [22 - 24]. However, several problems still need to be developed, namely the analysis of the fluid-structure interaction, the influence of position and the number of dentates on erosion. The complementarity of physical and numerical modeling is a very rich field to explore. The information obtained from numerical models is crucial for understanding the behavior of real structures and methods to design them effectively. Numerical modeling can help to interpret experimental results and thus reduce the number of physical modeling tests to be performed which are time-consuming and expensive, and determine data at any and all locations in the flow domain. The objective of this work is the development of a 3D numerical model with the commercial code LS-DYNA [10] using an SPH-FEM coupling method to simulate hydraulic phenomena of a reduced model of spillway type “Ski jump” with dentates. SPH method appears to be effective in solving diverse fluid-dynamic problems [25]. This relatively young method of calculation has some disadvantages such as a high computation time, especially in 3D simulations. In contrast to other studies, the purpose of this study is to adopt the SPH particle automatic generation method in LS-DYNA for creating the water flow by specifying the time and speed of particle injection. This method greatly reduces the complexity of the modeling process and the amount of

memory required for calculation. This work consists of numerically studying the flow at the outlet of the reduced model of the spillway for different scenarios of the location of dentates at different geometries. The feasibility of this numerical approach is shown by qualitatively comparing the numerical results with tests on a reduced physical model from the literature.

BASIC THEORY OF THE SPH METHOD

The ultimate objective of this study is to develop a numerical model which takes into account the fluid-structure interaction in order to simulate and allow better understanding of the free surface flow impacting a rigid plane in a reduced model of ski jump spillway. The SPH particle method will be briefly presented below.

This is a completely Lagrangian non-meshed method that consists of discretizing the domain into individual particles that interact with each other. This method has undergone strong developments in its precision and stability over the past decade for use in numerical fluid dynamics applications. The SPH method is able to solve complex problems such as high velocity impact, large material deformations and free surface flow.

The SPH formulation is based on a continuous integral representation of mathematical equations [11, 12]. This integral can be converted into discretized forms by summation over all particles in the domain of influence located inside the domain of the problem Ω (Fig. 1). The particle approximation for a function f associated with the position vector x at the level of a particle i is given by:

$$f(x_i) = \sum_{j=1}^N f(x_j) W_{ij} \omega_j \quad (1)$$

with

$$\text{with } W_{ij} = W(x_i - x_j, h) \quad (2)$$

N is the number of particles in the domain of influence of particle i and ω_j is the weight associated with each particle j . W is the kernel function defined on a compact support (domain of influence located in the domain of the problem). There are different possibilities for interpolation functions in the literature.

In Fig. (1), the ratio $h_t = K.h$ relates the radius of the support of the nucleus to the smoothing length (h) and to the kernel factor (K) which makes it possible to control the number of particles to be taken into account in the approximation. r_{ij} is the distance between particles i and j .

Turbine Swirling Device Effect on LPG-H₂ Engine In-Cylinder Flow Motion at Intake Stroke

Sahar Hadjkacem¹, Mohamed Ali Jemni^{1,*}, Zied Driss^{1,*} and Mohamed Salah Abid¹

¹ *Laboratory of Electromechanical Systems (LASEM), National School of Engineers of Sfax (ENIS), University of Sfax (US), Sfax, Tunisia*

Abstract: The main issue of internal combustion (IC) engines is efficiency. Engine inlet systems should be carefully designed to provide an optimum flow to the cylinder. Inlet manifold design is one of the ways to increase efficiency. This study focuses on improving the inlet system of an LPG-H₂ fueled engine by adding a static inclined blade turbine. It is a horizontal rotational axis turbine with four blades evenly distributed with an angle of inclination of 35°. Computational Fluid Dynamics (CFD) simulations are used in order to capture the in-cylinder flow motion and its influence on the flow characteristics. The method is assessed by application to flow calculations in the intake manifold for 3000 rpm engine speed. The percentage of supplied Hydrogen with LPG is equal to 20% in volume. The simulation results of in-cylinder turbulence kinetic energy (TKE), velocity and swirl motion were presented and discussed. Numerical results reveal significant improvements in the in-cylinder flow velocity, in-cylinder swirl motion and turbulent characteristics using an inlet system with a static swirling turbine (SST). Hence, this research found that by using a static turbine, we can improve the in-cylinder flow characteristics of the CI engine running with the LPG-20%H₂ blend.

Keywords: Engine, Flow, Hydrogen, In-cylinder, Inlet system, LPG, Swirl device, Static turbine.

INTRODUCTION

Due to the fast depletion of fossil fuels and an increase in the demand of energy with clean environment, the role of existing internal combustion engines needs to be reviewed now in the context of these two major crises. Hence, it is essential to explore other resources of energy. Renewable energy sources could be seen as a solution for sustainable energy [1, 2]. Wind energy is a promising renewable

* **Corresponding authors Mohamed Ali Jemni and Zied Driss:** Laboratory of Electromechanical Systems (LASEM), National School of Engineers of Sfax (ENIS), University of Sfax (US), Sfax, Tunisia

energy resource to help fight against global warming and environmental pollution from fossil fuel utilization [3]. In the transport sector, alternative fuels including gaseous fuels such as hydrogen [4 - 6], Compressed Natural Gas (CNG) [7], and Liquefied Petroleum Gas (LPG) [8], and biofuels such as biogas and biodiesel [9 - 11] are being experimented. However, conversion of a conventional engine into a gas engine can reduce the engine efficiency [12, 13].

The inlet system is one of the basic systems in the internal combustion engine [14]. It is the system that is liable for air-fuel blends to work into the block cylinder system to perform the combustion phase. In-cylinder flow motion during the intake, the stroke of an IC engine is one of the important factors, which governs its performance. The in-cylinder flow characteristic is affected by the geometry of the intake manifold since the flow path is created by the inlet of the intake manifold to the in-cylinder. Improvements in engine efficiency can also be attained by improved in-cylinder flow motion using an optimized intake manifold [15, 16]. A well-designed intake manifold will increase the swirl which is the rotation of charge about the cylinder axis. It is used in SI engines to enhance the scavenging process, liner cooling, and the mixing of the fuel with the air [17].

Some studies have been conducted on intake manifold design to enhance in-cylinder flow characteristics. Ceviz *et al.* [18], Hadjkacem *et al.* [19] and Jemni *et al.* [20] investigated the effect of intake manifold plenum length for different engine speeds on engine efficiency. They found that the use of a variable length plenum improves the engine's volumetric efficiency. Several researchers worked on piston geometries to optimize engine parameters. Harshavardhan *et al.* [21] found that a flat-with-center-bowl piston resulted in an improvement in the tumble ratio and turbulent kinetic energy of in-cylinder flows. Kumar [22] proved that modified pistons are better in terms of performance, combustion and emissions characteristics. Abdalla *et al.* [23] analysed the effects of adding a swirl generator to the intake manifold on engine performance. They proved that the engine with a swirl generator intake manifold has a greater torque, better BSFC and increased HC and CO emissions.

According to the above literature, so far not much research has been carried out to analyze the connection between the swirl device and the LPG-H₂ blends engine. In this direction, the main objective of this chapter is to study the influence of adding turbine in inlet system on in-cylinder flow characteristics of Clio2 LPG-20% H₂ fueled engine at 3000 rpm. The addition of the static turbine directly influences the nature and the homogenization of the mixture because of the turbulent movement created. In-cylinder swirl motion and turbulent kinetic energy are examined in the numerical process.

NUMERICAL APPROACH

In this work, a Clio2, four-stroke LPG-20%H₂ fueled engine has been considered for the CFD analysis. This research utilized CFD software, SolidWorks Flow Simulation (SWFS), to construct the engine inlet system CFD simulation. The inlet system is composed of an air filter, an intake throttle, an intake manifold, an engine head pipe, an intake valve, and a combustion chamber. Two inlet system geometries are proposed: with and without the emerged turbine. Its shapes were modeled using the SolidWorks Computer Aided Design “CAD” commercial code. SWFS has the advantage of importing the desired geometry directly from the CAD software to study the in-cylinder flow characteristics.

In the engine operation, the in-cylinder flow is turbulent and compressible. So, the averaged Navier-Stokes equations are used to predict the turbulent flows. These equations are illustrated in the appendix. The standard $k-\epsilon$ turbulence model is used. It is the most common model in the study of the in-cylinder gas flow engine [1].

GEOMETRICAL MODEL

Two inlet system geometries were modeled in this study using Solidworks: with and without static swirling turbine (SST). Fig. (1) demonstrates the inlet system with “SST”. It is a horizontal rotational axis turbine, placed at the intake manifold. Its outer diameter is 30 mm. As shown in Fig. (1), there are four blades evenly distributed with an angle of inclination 35° [24].

BOUNDARIES AND INITIAL CONDITIONS

The boundary and initial conditions used in the numerical study are defined according to the experimental measurements in a previous work [4]. In order to simplify the calculations, the cylinder walls were considered adiabatic. Only the fourth cylinder was in aspiration (critical cylinder). Pressure entrance was used in Fuel-orifice and air-filter entrances of the intake manifold equal to 1.013 bar (Fig. 2). Along the intake stroke, an alternative piston speed was taken as the output condition. In this study, the piston speed is calculated for a crank angle $\theta = 100^\circ$ after top death center “TDC”. At this stage, the piston speed is equal to the maximum value of 9.34 m/s and the intake valve is fully open with a maximum lift. The percentage of hydrogen in the mixture is 20% of H₂ and 80% of LPG [4].

Artificial Neural Networks Approach for Cross-Flow Heat Exchanger Fouling Modeling

Rania Jradi^{1,*}, Christophe Marvillet² and Mohamed Razak Jeday¹

¹ Research Laboratory, Process, Energy, Environment and Electrical Systems, National Engineering School of Gabes (ENIG), University of Gabes, Gabes, Tunisia

² CMGPCE Laboratory, French Institute of Refrigeration (IFFI), National Conservatory of Arts and Crafts of Paris (CNAM), Paris, France

Abstract: The traditional estimation methods such as fundamental equations, conventional correlations or developing unique designs from experimental data through trial and error have limits in thermal engineering due to the complexity of problems addressed. Thereby, the purpose of the present work is to explain the effective utilization of the Artificial Neural Networks (ANN) model in heat transfer applications for thermal problems, like fouling in a heat exchanger. The application of the ANN tool with different techniques and structures shows that it is an effective and powerful tool due to its small errors in comparison with experimental data. The feed-forward network with backpropagation technique was implemented in this study. Based on sensitivity analysis, the performance of the network trained was tested, validated and compared to the experimental data. The results achieved by sensitivity analysis show that ANN can be used reliably to predict fouling in a heat exchanger.

Keywords: Artificial neural network, Experimental data, Fouling, Fouling resistance, Heat exchanger, Heat transfer, Modeling.

INTRODUCTION

The application of black-box models such as artificial neural networks is emerging as a successful technique in various fields such as thermal analysis of heat exchangers during the last two decades. These techniques are recently used as a tool to modeling of heat exchangers, to estimate heat exchanger parameters, and phase change characteristics in heat exchangers and to control the heat exchangers [1].

* Corresponding author Rania Jradi: Research Laboratory, Process, Energy, Environment and Electrical Systems, National Engineering School of Gabes (ENIG), University of Gabes, Gabes, Tunisia; E-mail: raniajradi@yahoo.fr

The algorithms used in this field are characterized by simple models inspired from human intelligence and evolutionary experience. The classical methods used to estimate fouling resistance in heat exchangers that include using fundamental equations, employing conventional correlations, or developing unique designs from experimental data through trial and error have limits due to the complexity and the non-linearity of the problem. To overcome this difficulty, a simple artificial neural networks (ANN) method can be implemented based on databases available from experimentation. In comparison with classical estimation methods that need a definition of correlations and an iterative method, this method needs only input/output samples for training a special neural network, in turn, obtaining output results as test samples fed into the trained network. Among the main advantages of this technique are an accurate approximation of complex problems, greater efficiency than phenomenological models even for multiple response computations, and greater effectiveness even with incomplete and noisy input data.

Fouling in heat exchangers is among the serious and complex problems encountered for decades in industry, which reduces the performance of these equipment [2]. It is defined as the accumulation of any undesirable deposit on the heat exchanger surfaces [3].

Fouling resistance is a numerical indicator for the product of the thermal resistance by the heat exchange surface. This indicator is equal to 0 if the heat exchanger is new and increases progressively over time when the solid materials get deposited on the walls of the heat exchanger until this equipment is cleaned [4].

Fouling poses several problems in the operation of heat exchangers and inevitably induces significant additional costs mainly due to the increase in energy consumption, production losses, and cleaning and maintenance costs associated with plugging and clogging of pipes [4]. It represents an added thermal resistance which reduces energy performances [5].

ANN approach has been successfully employed as a prediction model of fouling resistance in various types of heat exchangers for planning suitable cleaning schedules and for controlling operation of the process [3].

Davoudi and Vaferi [5] developed an efficient model to estimate the fouling factor for both single tube heat exchanger and annular heated probe using ANN. The developed model links a fouling factor to independent operating variables of the portable fouling research unit by means of the Multilayer Perceptron (MLP) network tool. The independent operating variables used in this work comprised seven parameters, which are density, surface and fluid temperature, diameter of

fluid passage, velocity of fluid, the concentration of dissolved oxygen in fluid and time.

Mohanty [6] applied ANN for heat transfer analysis of a shell and tube heat exchanger subjected to fouling. This research recommends the use of ANN methodology to predict performances of a shell and tube heat exchanger in industrial applications.

In the same context [7], some researchers applied the Nonlinear Auto-Regressive system with an exogenous network to predict the fouling resistance in shell and tube heat exchangers. The proposed integrated approach accounts for an alternative to optimize operating conditions and preventive maintenance of heat exchangers.

Sundar *et al.* [8] developed an accurate and generalized deep neural network framework capable of predicting overall fouling resistance and individual flue-gas side and water-side fouling resistance of a cross-flow heat exchanger used in waste heat recovery. The authors provide a robust algorithm framework for fouling prediction that can be generalized and scaled to various types of industrial heat exchangers. More recently, Jradi *et al.* [3] used artificial neural networks for both shell and tube and cross-flow heat exchangers to predict the fouling resistance in order to plan suitable cleaning schedules and to control operation of the phosphoric acid concentration plant.

In this context, the present work aimed to present the ANN structure, methodology and implementation in the case of heat exchanger fouling problem. This work will encourage the thermal engineers to consider ANN to deal with critical heat transfer problems which are difficult to treat by conventional methods.

ARTIFICIAL NEURAL NETWORK STRUCTURE AND METHODOLOGY

The use of an artificial neural network which is a new approach allows the investigation of several competing hypotheses simultaneously for linear and non linear system with high complexity in various engineering fields [9]. It is also used to control dynamic and aging processes such as fouling. An artificial neural network is composed of a large number of highly interconnected processing elements called artificial neurons which are joined by connecting links. A value is assigned to each link called weight, which allows communication between neurons. The best efficient design of artificial neural network is based on the choice of the three layers, the number of neurons in the hidden layer, the transfer function, the number of hidden layers and the learning algorithm [10]. The

CHAPTER 6

The Effect of the Nitrogen Percentage on the Microstructure and Mechanical Properties of Zr-N Coatings

Linda Aissani^{1,2}, Nourredine Belghar^{3,*} and Zied Driss⁴

¹ Department of Mater Science, Abbès Laghrour University of Khenchela, Khenchela, Algeria

² Laboratory of Active Components and Materials, Larbi Ben M'hidi University of Oum El Bouaghi, Oum El Bouaghi, Algeria

³ LGEM Laboratory, University of Biskra, Biskra, Algeria

⁴ Laboratory of Electromechanical Systems (LASEM), National School of Engineers of Sfax (ENIS), University of Sfax (US), Sfax, Tunisia

Abstract: Nitride-based hard coatings have attracted increasing interest over the last decades for machining, and cutting tool applications, owing to their high hardness, high thermal stability, good wear, and corrosion resistance. In this work, we investigated the effect of nitrogen concentration, as a reactive gas, on the structure and properties of Zr-N coatings deposited by magnetron sputtering. The structural and morphological properties of Zr-N films were described, followed by a detailed investigation of the mechanical properties of Zr-N coatings. By varying the nitrogen percentage, the structure and the hardness of Zr-N films were evaluated in a wide range. With a rising N₂ percentage, the structure changed from Zr₂N at 10% N₂ to a mixture of Zr₂N and Zr N from 20%N₂ with the NaCl_{B1}-type structure. Insertion of nitrogen atoms on the Zr leads to significant changes in film microstructure, grain size, and surface morphology, as evidenced by x-ray diffraction, scanning electron and atom. The hardness of the films was first augmented by increasing the nitrogen percentage and take a maximum value was 22 GPa for the films deposited under 20%N₂ then decreased.

Keywords: Hard coating, Magnetron sputtering, Microstructure, Nitride, PVD, Reactive gas, Steel, Thin films, Zr-N.

INTRODUCTION

The metal nitrides, M-N (Me = early transition metal), belong to a specific class of materials that is gaining importance because of their high potential to be used for protective applications in severe conditions. They are very hard, have good

* Corresponding author Nourredine Belghar: LGEM Laboratory, University of Biskra, Biskra, Algeria; E-mail: n.belghar@univ-biskra.dz

thermal conductivity and good corrosion and wear resistances [1]. Among them, Zr nitrides are very well-known materials widely applied as hard wear-resistant protective coatings for cutting tools and other components [2, 3].

The zirconium alloy is widely used in nuclear reactors as a fuel cladding material or for research reactor reflector vessels because of its attractive combination of low neutron absorption cross-section, good corrosion resistance, and high hardness [4]. However, the formation of fragile pure Zr during service will result in a fragile phase with a high fracture toughness of the material. Moreover, Zr is susceptible to a crack initiation and propagation process in the film surface that potentially reduces its usable lifetime [4]. The precipitation of Zr in the alloys can influence by several factors, including the microstructure, residual stresses and temperature gradients [5]. So far, research on the precipitation and distribution of Zr in the alloys as a fracture initiator has received considerable attention [5]. The addition of Nitrogen to Zr enhances mechanical properties and significantly improves the oxidation resistance due to the formation of a dense ZrN phase. ZrN is a refractory interstitial nitride with a golden color, high hardness, high corrosion resistance, and relatively high conductivity.

ZrN exhibits a covalent bonding due to interactions between the 2s state of the N and 4d state of Zr, resulting in Zr–N bonding. ZrN can accommodate non-metal vacancies, and their non-stoichiometric formula can be written in other phases like Zr_2N and Zr_3N_4 , respectively. Due to the structure and bonding, Zr-based coatings exhibit a large range of useful properties such as good conductivity, high hardness, high-temperature point, biocompatibility, excellent resistance to wear, corrosion and oxidation, rendering them suitable candidates for use in biomedical, corrosion-resistant, nuclear, electrical and decorative applications and modeling and computational analysis [6].

The properties of ZrN are affected by nitrogen fraction and impurities, especially oxygen, as a small amount of oxygen may form unwanted titanium oxides, which may lead to an imbalance in optical properties, hardness and conductivity. ZrN films with different nitrogen contents were prepared to analyze the structural and mechanical features. At a high flow rate, the nitrogen content first high slowly from 0 to 5 at %; additionally, the increase of nitrogen flow rate leads to a steep high of the coating nitrogen content up to 48 at %; which corresponds to the stoichiometric fcc-ZrN phase. XRD diffraction showed the development of the hexagonal Zr phase with a strong (002) orientation, where the N atoms taken octahedral sites in the Zr lattice as the quantity of Nitrogen is increased; for nitrogen contents of 20 and 30 at.%, the hc- Zr_2N phase have a (200) preferential orientation. At higher nitrogen content, the fcc-ZrN phase becomes predominant. When nitrogen content rises, the films become more solid and range from

approximately 8 GPa for pure Zr to 19.0 GPa for a nitrogen content of 48 at.%. The hardness remains constant with a value of approximately 19.0 GPa within the range of 42 and 48 at. % N. This is mainly affected by the structure, the lattice deformation and the increase in stresses. Hardness increases nearly linearly with rising stresses, indicating that lattice deformities and the corresponding increases in intrinsic stresses are important factors for the hardening of the coating [7].

In spite of all these research [7, 8], the knowledge available is still insufficient to provide a quantitative description of the influence of these deposition parameters, and the correlation between the microstructure, morphology, and the mechanical of based Zr phases has led to intensive study in order properties of the ZrN and their interaction with the other elements is still not well known. On the other hand, the formation of different based Zr phases in the ZrN films has been conducted *via* various techniques such as X-ray Diffraction, EDS, and XPS [9]. Sufficient information in terms of the phase, morphology, and size of ZrN and the orientation relationship between the structural and mechanical properties, can be derived from these investigations. For example, the thin films of ZrN deposited have been done directly by XRD [9]. Owing to the restricted areas of thin films, the formation of different mixture phases on the thin films cannot be well examined.

Hence, the aim of this work is to evaluate the Zr-N coatings deposited by magnetron sputtering and demonstrate the influence of the nitrogen content on their structural and mechanical properties.

Experimental Detail

Zr-N films were deposited on Si(100) wafers (10 mm×10 mm×480 μm) and XC100 (Ø 30 mm × 3 mm) substrates through the reactive magnetron sputtering method (DEPHIS 4, Etupes, France) [2]. In this experiment, we used Si (100) (10 mm×10 mm×480 μm) to determine the chemical commotions and surface morphology and film thickness, and XC100 (Ø 30 mm × 3 mm) substrates to determine the mechanical property. The schematic of the deposition procedure is presented in Fig. (1).

A sputtering film with a pure Zr target (99.99% purity, D = 10 cm diameter, e = 6 mm) was operated at 550 W in the sputtering process under different nitrogen flow rates and a sputter time of 180 min. The total flow rates of Ar and N₂ were fixed at 100 sccm with a working pressure of 0.4 Pa. The target-to-substrate distance was 10 cm. The substrates were polished and cleaned in acetone and ethanol, dried, and then fixed on the substrate-holder. Prior to the film deposition, the Zr target was etched by Ar ions bombardment for 5 min. The films were

Non-Newtonian Pseudoplastic Fluid Flow and Heat Transfer inside a Horizontal Duct: New Correlations

Horimek Abderrahmane^{1,*}, Abed Saad¹ and Ait-Messaoudene Nouredine²

¹ Department of Mechanical Engineering, Ziane Achour University, Djelfa, Algeria

² Laboratoire des Applications Énergétiques de l'Hydrogène (LApEH), Blida University 1, Blida, Algeria

Abstract: In this chapter, we have studied the problem of forced convection in a simple horizontal cylindrical pipe. Two boundary conditions are considered, uniform constant heat flux and uniform temperature. The fluid to be heated is pseudoplastic, modeled by the Ostwald law ($n \leq 1.0$). A fully developed velocity profile is assumed at the pipe entrance. The energy equation is solved numerically with a simple implicit finite difference scheme. Results focus on the effects of the rheological behavior (index n), the type of heating, and the Pe number on the heat transfer coefficient (Nu) and the thermal entry length. They show an improvement in heat transfer with a decrease in the fluid-structure index (n). An increasing thermal length when Pe and/or n increase is also recorded. This may lead to a huge increase in the tube's length when a thermal establishment is targeted. New, simple, precise, and physically indicative correlations with wide ranges of variation of the main parameters are proposed here. Their mathematical forms are chosen mainly to guide manufacturers for heat exchangers dimensioning. Scientists have also shown an interest in them as tools for validation and physical interpretation.

Keywords: Correlations, Cylindrical horizontal duct, Forced convection, Imposed heat flux, Imposed temperature, Pseudoplastic fluid.

INTRODUCTION

Heat exchangers are essential equipment in the industrial sector. They can be designed by simple circular tubes, annular, and with more or less complex geometries. They can be small like those in electronic devices or very large as in nuclear power plants. Their dimensioning sometimes makes their study very tiring and expensive, especially for special fluids. Among the fluids supposed to go

* Corresponding author Horimek Abderrahmane: Department of Mechanical Engineering, Ziane Achour University, Djelfa, Algeria; E-mail: Horimek_aer@yahoo.fr

through the heat exchangers, many of them have a non-Newtonian behavior. For instance, we can cite pasta dough that is heated to be later sterilized; hence there is a need to perfectly control its temperature at the exit of the exchanger to ensure correct sterilization. We can also mention paper pasta pulp, chemical products, and so on. Exchangers' Design Engineers must master the process of heating with perfect knowledge of fluid types. The pipe length (a key element of a heat exchanger sizing) should be determined accurately. Usually, we look for the establishment point, *i.e.*, the thermal entrance length. The fully developed part of the pipe is extensively studied in the literature, and a lot of simplifications are made. However, for non-Newtonian fluids, the design that must go through numerical solution procedures is not within reach of all engineers. For this type of fluids, it is preferable to work with correlated formulas based on those procedures, where their validity limits may vary according to needs and skills.

For this purpose, thermal development forced convection along a simple cylindrical tube will be studied here. The dynamic flow (velocity profile) is assumed to be known at the entrance region. This type of problem is well-known as Graetz's problem [1]. His work has led to a simplified form of the energy equation. It was only later that the equation developed by Graetz was solved analytically by W. Nusselt [2], using the technique of variable separation. Thus, many scientists name it as Graetz-Nusselt problem. It should be noted that the first considerations were very simple. Hundreds of works have been carried out since then and are still being continued, raising complications that were not possible earlier. Identifying all the published works on Graetz's problem is an impossible task; for this purpose, we will summarize a few works that are close to our work and help better understand our study. From the previous details, the present study is interested in the same problem (Graetz), where we evaluate the effects of the rheological index n (describing the non-Newtonian behavior) and the Peclet number Pe on the heat transfer rate along with the determination of the thermal length.

For the case of Newtonian fluids, Sellars *et al.* [3] and Siegel *et al.* [4] considered the problem of forced convection through a cylindrical pipe in a situation of uniform flux imposed on the wall with the same assumptions made by Graetz. The effect of axial conduction was analyzed by Hsu [5], where the problem was solved analytically by the separation of variables method. Cheng and Ou [6] resolved the same problem by considering the effects of viscous dissipation. A. Barletta [7] discussed the effect of viscous dissipation along with an infinitely long circular pipe, where the wall is subjected to an axial distribution of heat flux. In a subsequent work [8], the author considered three types of flux distribution in order to ensure that there is an asymptotic region invariant for the Nusselt number. Barletta and Zanchini [9] considered a problem similar to the earlier two

by exposing the pipe to three types of heating; a constant flux, a linearly varying flux along the tube, and finally, a flux with an exponential axial variation. The authors solved the system of equations analytically and through the use of the Laplace transform technique. Numerous graphs for the Nusselt Number (Nu) were provided. O. Aydin [10] analyzed the same problem, taking into account the effect of viscous dissipation. Two boundary conditions were considered: constant flux and imposed constant temperature. The radial temperature distribution and the Nusselt number were determined for different values of the Brinkman number for both heating cases. Sun and Kakas [11] treated the problem numerically using the finite volume method. Three thermal conditions on the wall were considered: constant temperature, the temperature varying linearly along the axis, in addition to the case of constant flux. The effect of viscous dissipation has been taken into account.

For the case of non-Newtonian fluids, Khelaff and Lauriat [12] studied the problem of forced convection in a circular pipe and between two parallel plates for a fully developed flow (dynamically and thermally) in the case of an Ostwald fluid (also called Ostwald-De-Waele fluid). The authors used the method of variables separation based on the evaluation of eigenvalues and eigenfunctions. Cotta and Ozisik [13] presented a theoretical study on forced laminar convection in a circular duct and between two parallel plates for imposed temperature as a heating condition. The authors treated this problem using the Eigenfunctions technique to determine Nusselt evolution and bulk temperature distribution for a fluid described by the power-law model. Three values of the index n were considered: $n=3$, 1, and $1/3$. The obtained results for local Nusselt number in the case of parallel plates were compared with those obtained by S. M. Richardson [14]. In the case of a circular pipe, the results were compared with those of Bird *et al.* [15]. Patrikh and Mahalingam [16] analytically studied the thermo-convective transfer of a pseudoplastic fluid flow ($n=0.555$ and 0.71) in a circular duct, under similar heating conditions, initially with constant flux and subsequently with arbitrarily varying flux. Duhamel's principle and Siegel's approach formed the basis of their work. The main object of the study was to determine wall temperature. The obtained results were compared with those obtained experimentally, and they showed good agreement.

However, for a power-law model fluid, A.R. Mansour [17] studied the problem in a circular duct under constant temperature. The technique of separating variables, combined with Laplace transformation, was used for solving the equations. The effect of the n index on the heat exchange rate (Nu) has been well illustrated by many graphics. A. Barletta [18] studied the asymptotic behavior of the temperature field for a case similar to that in a previous study [17] by taking the viscous dissipation into account. On the wall, he assumed a constant flux which

CHAPTER 8**Design, Mathematical Modeling and Thermal Performance Evaluation of Water Solar Collector for the Desalination Process****K. Zarzoum^{1,*}, K. Zhani² and H. Ben Bacha³**¹ *LASEM (Electromechanical Systems Laboratory), National Engineering School of Sfax, Sfax University, Sfax, Tunisia*² *Department of Mechanical Engineering, College of Engineering, University of Bisha, Bisha, Kingdom of Saudi Arabia*³ *Department of Mechanical Engineering, College of Engineering at Alkharj, Prince Sattam Bin Abdulaziz University, Alkharj, Kingdom of Saudi Arabia*

Abstract: This chapter presents the modeling and the experimental study of a water solar collector coupled to an optimized solar still developed in order to boost freshwater production in a solar distillation system. The desalination process is currently operated under the climatological conditions of Sfax, Tunisia. To numerically simulate the water solar collector, we developed a dynamic model based on heat and mass transfer of the water solar collector. The obtained set of ordinary differential equations was converted to a set of an algebraic system of equations by the functional approximation method of orthogonal collocation. The aim of this study is to present the mathematical model and experimental study of this water solar collector.

Keywords: Condensation, Desalination, Evaporation, Experimental investigation, Humidification, Solar still.

INTRODUCTION

Solar energy heaters are heat exchangers that convert incoming solar energy into internal energy of the transport medium, in this case, seawater. The function of the solar heater within the distillation unit is to ameliorate the outlet water temperature of incoming swab water to a determined temperature that will allow the operation of the evaporator unit and the separation of feed-fresh water from thick swab-rich water. The water solar heater, the object of this study, is one of five components (air solar collector, water solar collector, humidifier, solar still

* **Corresponding author K. Zarzoum:** LASEM (Electromechanical Systems Laboratory), National Engineering School of Sfax, Sfax University, Sfax, Tunisia; E-mail: kamelissat@hotmail.com

and inner condenser) of an optimized solar still system, as shown in Fig. (1). The solar desalination system is grounded on the air humidification and dehydration principle. The SS is a simple system and provident process using solar energy to produce fresh water. Several designs and a lot of studies have been developed to meliorate the productivity of solar stills. A SS system was tested with an energy storehouse media at its base by Naim and Abd El Kawi [1]. The performance of a solar still system with different size sponger cells placed in the water receptacle was studied experimentally by Bassam and Himzeh. Murugavel and Srithar [2, 3] presented an experimental study of an optimized SS with different depths of water in the receptacle and different wick accouterments like cotton cloth and sponger distance. Yadav and Yadav [4] studied the SS by incorporating reversed absorber asymmetric line-axis emulsion parabolic collector and concluded that the distillate water was increased in comparison to conventional SS. This is because the SS entered solar energy both from the top and nethermost, increasing the temperature difference between the water face and glass cover. The colorful factors affecting the productivity of a solar still coupled with a solar heater and the influence of inclination of the water heater of a conventional SS system were optimized by Tanaka and Nakatake [5]. Zaki *et al.* [6] presented an experimental study of active solar still integrated with a solar water collector and plant where the maximum increase in the yield was over 33.

Ahsan and Fukuhara [7] introduced a new model of heat and mass transfer of a tubular SS system. They show that the heat balance of the sticky air and the mass balance of the water vapor in the sticky air were formalized for the first time. Sakthivel *et al.* [8] presented an experimental study of a modified SS system by adding jute cloth in a perpendicular position in the middle of the receptacle and another row of jute cloth attached to the still wall. A vertical shaft rotating by a small wind turbine and inclined SS were integrated with the main device of solar still system as a mongrel system of distillation studied by Eltawil and Zhengming [9]. They show that the inclined water still produced a better yield than that of the SS main device by roughly 29.17. Arslan [10] delved into the performance of colorful designs of active SS under an unrestricted cycle mode experimentally and concluded that the indirect box active SS design produced the loftiest overall diurnal edge. Also, El-Sebaili *et al.* [11] delved into a new fine model to study the thermal performance of the SS with phase change material. El-Zahaby *et al.* [12], presented a new conception of a SS coupled to a flashing chamber to meliorate the freshwater yield. Bacha and [13], Zarzoum *et al.* [14 - 16] and Mokhless Boukhriss *et al.* [17] designed a new SS with an energy-storing material in the water receptacle to extend the operation of the distiller at night. They also integrated a water and air solar heater and a separate condenser coupled to the SS system to meliorate the productivity. Zeinab and Ashraf [18] developed a rotating shaft with a vertical axis introduced near the water face of the absorber of SS

system to meliorate the diurnal productivity. They coupled this SS to an electrical motor to rotate the shaft. They show that this new design of the SS was bettered by 5.5 in July, 5 in June, and 2.5 in May. Badran and Tahaine [19] developed SS by adding glasses on the interior walls and coupled them with a solar collector experimentally. This work presented a fine modeling and an experimental study of the water solar heater coupled with the optimized SS in Sfax, Tunisia.

Based on the literature, the solar desalination system under study differs from the previously published works by using a humidifier and an evaporation tower, on the one hand, and a field of flat-plate air solar collectors and a field of flat-plate water solar collectors on the other, which make the system more flexible and increase the freshwater production. A synoptic schema of the humidification-dehumidification process is presented in Fig. (1). Sea or brackish which is preheated in the condensation tower, by the latent heat of condensation, and heated in the water solar collectors is pulverized into the humidifier and the evaporation tower.

Due to heat and mass transfers between the hot water and the heated airstream in the humidifier in case of working in a closed air loop and between the hot water and the ambient air stream in the evaporation tower in case of working in open air loop, the latter is loaded by moisture. To increase the surface of contact between air and water, and therefore to raise the rate of air humidification, a packed bed is implanted in the tower of evaporation and the humidifier. The saturated moist air is then transported toward the tower of condensation, where it enters in contact with a surface whose temperature is lower than the dew point of the air.

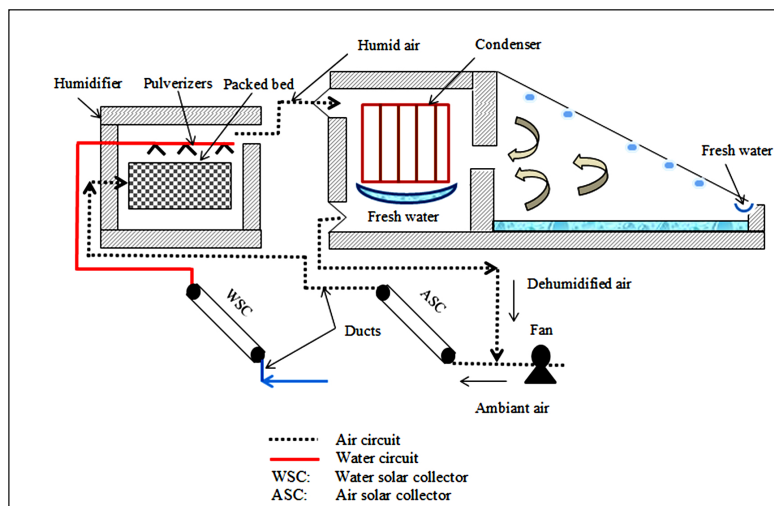


Fig. (1). A schematic diagram of the experimental setup.

Structural and Mechanical Properties of Ti-N Films – Abinitio Calculations and Experiment

Sara Fares¹, Linda Aissani^{2,3}, Abdehak Ayad^{1,4}, Nouredine Belghar^{5,*} and Zied Driss⁶

¹ *Laboratoire Microstructures et Défauts dans les Matériaux, Université Frères Mentouri Constantine 1, Route Ain El Bey, Constantine, Algeria*

² *Department of Matter Sciences, Abbès Laghrour University of Khenchela, Khenchela, Algeria*

³ *Laboratory of Active Components and Materials, Larbi Ben M'hidi University of Oum El Bouaghi, Oum El Bouaghi, Algeria*

⁴ *Département de Pharmacie, Faculté de Médecine. Université Salah Boubnider Constantine 3 Nouvelle ville Ali Mendjeli, Constantine, Algeria*

⁵ *LGEM Laboratory, University of Biskra, Biskra, Algeria*

⁶ *Laboratory of Electromechanical Systems (LASEM), National School of Engineers of Sfax (ENIS), University of Sfax (US), Sfax, Tunisia*

Abstract: In this work, we investigated the effect of film thickness on the structure and properties of Ti-N films deposited by magnetron sputtering. The structural properties of Ti-N films were described, followed by a detailed investigation into their mechanical properties by using theoretical and experimental analysis. The theoretical calculation presented the Rocksalt TiN structure with a lattice parameter of about 4.255 Å, confirmed by X-ray diffraction. The experimental analysis revealed that the structure and the hardness of TiN films varied in a wide range when increasing the film thickness. The structure morphology also changed from a rough to a dense surface and a smooth structure. The hardness and Young modulus of the TiN film reach maximum values of about 26 GPa and 445 GPa, respectively, and then decrease with increasing the film's thickness. The theoretical values of the hardness and young modulus are in excellent agreement with those obtained for the Ti-N thick films.

Keywords: DFT, Film thickness, Hard coating, Index terms, Magnetron sputtering, Mechanical properties, Microstructure, Nitrogen, PVD.

* **Corresponding author Nouredine Belghar:** LGEM Laboratory, University of Biskra, Biskra, Algeria; E-mail: n.belghar@univ-biskra.dz

INTRODUCTION

In recent years, there has been significant development of hard nitride film coatings for several technical fields [1, 2]. The physical and mechanical properties of rocksalt-structure transition-metal nitrides (Ti, Cr, Zr, V...), such as their high hardness, chemical stability, high melting point, and excellent electrical and thermal conductivity, make them attractive for technological applications [3 - 5]. According to their applications, a better understanding of the interdependence between their properties influences the choice of films significantly. Rocksalt, a basic structural prototype, turns out to be the most stable of several different structures. A significant amount of effort has also been put into searching for new transition metal nitrides with extreme hardness and high fracture toughness, with the expectation that many of them may find use in cutting tools and hard coatings. Among these metal nitrides, titanium nitride (TiN) with adequate biocompatibility is regarded as an essential biomaterial [6 - 9].

TiN coatings are widely used as protective coatings to improve the performance of cutting or friction tools. The high hardness and low coefficient of friction characteristics of the coating combine to make the coating extremely profitable in reducing overall wear. These coatings are not limited only to cutting tools because their resistance to wear and corrosion are properties that find applications in other fields: dental instruments, surgical implants, forging molds and dies, gears, valves, or decorative elements [5, 10, 11].

Elastic modulus and hardness are essential factors in predicting the wear and adherence of thin films on surfaces and their response to mechanical stresses. For this aim, a complete determination of the elastic properties of TiN binary has been established, including single-crystal elastic constants c_{ij} and elastic moduli (B, G, and E) of isotropic polycrystalline materials.

For a few years now, numerical simulations have acquired a place of choice in calculating the properties of thin films. Currently, it is possible to describe materials using theoretical models which can support experiments (or even replace them) and predict the behavior of materials where experience is lacking or that it is very expensive and sometimes difficult to achieve. The comparison of the results obtained with the available experiments makes it possible to validate the relevance of the theoretical approaches.

Several simulation techniques have been developed for calculating the different properties of materials, particularly the ab initio methods, which have become a fundamental tool for calculating the structural, electronic, magnetic, and elastic properties of complex systems [12]. For thin films, the first-principle calculations are generally carried out within the framework of density functional theory (DFT)

[13, 14]. S. Yu *et al.* [15] studied phase stability, chemical bonding, and mechanical properties of TiN films using DFT within the generalized gradient approximation (GGA) [16] and the local density approximation (LDA) [17]. The mechanical, structural, and tribological properties of titanium nitride by a pulsed laser were studied by Ettaqi *et al.* [18]. The elastic properties and thermophysical properties of Ti (C1-xNx) alloys ($x=0-1$) were also investigated using ab initio DFT total energy calculations [19]. Kim *et al.* [20] also used the full ab initio method to calculate the color of TiN ad ZrN, which includes both interband and intraband transitions Kim *et al.* [20] calculated the color of TiN ad ZrN, which includes both inter-band and intra-band transitions using the full ab initio method to calculate.

COMPUTATIONAL DETAILS

The present simulation is based on the density functional theory (DFT), which is one of the most accurate theories for calculating the electronic and structural properties of solids [21], with first-principles calculations performed within the full-potential linearized augmented plane wave (FP-LAPW) method [22] using the WIEN2k code [23]. First, we will start with the structural properties. The crystal structure of the NaCl phase can be defined by the lattice parameter a . The space group for this phase is 215 (Fm-3m). Ti and N are in FCC positions as follows: Ti (0.0.0) and N (1/2, 1/2, 1/2). For our binary compound, the values of the Muffin tin radii are considered equal to 1.98 and 1.70 Bohr, respectively, for Ti and N.

For the initialization, the exchange and correlation potential was calculated using the generalized gradient approximation (GGA) parametrized by Perdew-Burk-Ernzerhof (PBE) [16]. The space is divided into two regions in the FP-LAPW method: the first is a non-overlapping muffin-tin (MT) spheres region, where the basis set within this region is described by radial solutions of the one-particle Schrodinger equation and their energy derivatives multiplied by spherical harmonics. The second is an interstitial region (IR) plane wave that makes up the basic set [24, 25]. The convergence tests allow us to select the value $R_{mt} * K_{max} = 9$, where R_{mt} denotes the smallest atomic sphere radius and K_{max} denotes the plane wave cut-off [25]. The G_{max} value was chosen to be 14 when G_{max} is defined as the magnitude of the largest vector in the charge density Fourier expansion. Up to $l_{max} = 10$, the MT sphere was considered. The Monkhorst-Pack method used 1000 k points in the first Brillouin zone (IBZ). The charge convergence parameter was set at 10^{-4} .

Finally, mechanical properties were determined using IR Elast. The knowledge of the elastic constants C_{ij} provides important information about the crystal's

SUBJECT INDEX**A**

Ab initio methods 107, 108
 Absolute average relative deviation (AARD)
 58, 59, 61
 Aging processes 56
 Air 39, 42, 45, 46, 90, 91, 92, 93, 98, 100,
 101, 102, 109
 filter 46
 fuel blends 45
 humidification 90, 91, 93
 solar heater 90, 92, 98, 101
 Amplification factor 80
 ANN architecture 57
 Ansys-fluent, commercial software 5
 Applications 1, 28, 56
 industrial 1, 56
 numerical fluid dynamics 28
 Artificial neural networks 54, 56

B

Behavior 26, 27, 31, 48, 49, 74, 101, 107
 asymptotic 74
 hydraulic 26
 Block 21, 45
 cylinder system 45
 force vector 21
 Bragg formulas 109
 Brillouin zone 108
 Brinkman number 74, 75

C

CAD software 46
 Calculations 27, 28, 32, 46, 77, 80, 83, 106,
 108
 numerical 83
 theoretical 106
 total energy 108
 Cauchy 18, 21

 green tensor 18
 stress tensor 18, 21
 CFD analysis 46
 CO emissions 45
 Coating(s) 64, 107, 109
 adhesion 109
 hard nitride film 107
 nitrogen content 64
 Combustion 45, 46, 49
 chamber 46
 process 49
 Compressed natural gas (CNG) 45
 Computational fluid dynamics (CFD) 44, 48,
 50
 Conditions 74, 75, 80, 97, 101, 104
 meteorological 97, 101, 104
 thermal 74, 75, 80
 Constant 107, 110
 calculated lattice 110
 single-crystal elastic 107
 Constitutive equation 24
 Convection, forced laminar 74
 Correlations 54, 55, 65, 72, 75, 83, 84, 85, 86,
 108
 conventional 54, 55
 empirical 75
 Corrosion 63, 64, 107
 resistance 63
 Coupled SPH-FEM method 26
 Cubic cavity 2

D

Decorative elements 107
 Density 4, 13, 55, 58, 61, 78, 106, 107, 108
 functional theory (DFT) 106, 107, 108
 Dental instruments 107
 Dentate geometries 29
 Deposition 65, 68, 109
 duration 109
 procedure 65
 rate 68

Zied Driss (Ed.)

All rights reserved-© 2023 Bentham Science Publishers

Deposition conditions 66, 110
 for TiN films 110
 for ZrN films 66
Design, inlet manifold 44
DFT calculation 110, 112, 114
Diffuse elements method 16
Discrete element method 42

E

Elastic modulus 66, 107
 and hardness 107
 values 66
Elastic solids mechanics 16
Electrical motor 91
Electronic devices 72
Element-free galerkin method (EFGM) 15, 16,
 22, 24
Energy 44, 49, 80
 dimensionless equation 80
 sustainable 44
 turbulence kinetic 49
Engine 44, 45
 conventional 45
 gas 45
 inlet systems 44
Engineers 56, 73, 75, 83
 industrial 83
 thermal 56
Environmental pollution 45

F

Face-centered cubic crystal lattice 110
Field(s) 6, 21, 22, 27, 47, 48, 49, 50, 54, 55,
 91, 107, 110
 displacement 22
 emission scanning electron microscope 110
 technical 107
 thermal 6
Film 63, 65, 68, 70, 106, 109, 110, 111, 112,
 113, 114
 deposition 65, 109, 110
 microstructure 63
 thickness 65, 68, 70, 106, 111, 112, 113,
 114
Finite 5, 15, 24, 26, 27, 31, 41, 74
 element method 15, 24, 26, 27, 31, 41
 volume method (FVM) 5, 27, 74

Fluid 16, 72, 75, 76, 78
 mechanics 16
 pseudoplastic 72, 75, 76
 viscosity 78
Forces 7, 26, 32, 39
 hydraulic 26
Fouling 54, 55, 56, 57, 58, 59, 60, 61
 in heat exchangers 55
 resistance 54, 55, 56, 57, 58, 59, 60, 61
Fourier law 79
FP-LAPW method 108
Framework 25, 56, 107
 neural network 56
Friction 39, 107
 characteristics 107
 laws 39
 tools 107
Fuels 44, 45
 fossil 44
 gaseous 45

G

Geometric transformations 17
Graetz-Nusselt problem 73
Green deformation tensor 17, 18

H

Hardness and elastic modulus 66, 70
Heat exchange 2, 55, 86
 surface 55
Heat exchangers 54, 55, 56, 59, 61, 72, 73, 84,
 89
 cross-flow 56, 59, 61
 industrial 56
Heat transfer 1, 2, 54, 56, 72
 analysis 56
 applications 54
 coefficient 72
 properties 2
Heated block 1
Heater system 100, 101
 air solar 100, 101
Humidification-dehumidification process 91
Hydroelectricity 26
Hyperelastic law 18
Hyperelasticity 15, 16, 18, 21
 isotropic 18

I

Index, rheological 73, 77, 82, 86
 Inlet 44, 45, 46, 47, 49, 80
 effects 80
 system 44, 45, 46, 47, 49
 Insertion of nitrogen atoms 63
 Intake manifold 44, 45, 46
 generator 45
 optimized 45
 Interconnected processing elements 56

K

Kernel 28, 29
 factor 28
 function 28, 29

L

Laplace 74, 75
 transform technique 74, 75
 transformation 74
 Lattice deformation 65
 Liquefied petroleum Gas (LPG) 44, 45, 46

M

Mesh(s) 15, 32
 distortions 15
 explicit 15
 solid finite element 32
 Metal nitrides 63, 107
 Monkorst-pack method 108
 Moving least squares (MLS) 15, 16, 19
 Murnaghan's equation 31

N

Nanofluid 7, 8, 10
 density 10
 flow 7, 8
 Neurons 56, 57, 58, 61
 artificial 56, 57
 single 57
 Newtonian fluid 73, 75, 81
 and heated tube 81
 Nitrogen 63, 64

 concentration 63
 fraction 64
 Non-metal vacancies 64
 Nonlinear 15, 24, 56
 auto-regressive system 56
 computational method 24
 formulations 15
 Nuclear 64, 72
 power plants 72
 reactors 64
 Numerical 1, 5, 27, 33, 34, 101, 107
 method 5, 27
 modeling of spillways 27
 simulation in dynamic regime 101
 simulations 1, 5, 33, 34, 101, 107

O

Ogden's 15, 24
 hyperelastic materials 15
 law 24
 Ordinary differential equations (ODE) 89, 97
 Orthogonal terms method 97
 Ostwald 72, 74, 75
 fluid 74
 law 72, 75

P

Partial differential equations (PDE) 97
 Pipes 46, 55, 73, 74, 82
 engine head 46
 heated 82
 Plant 56, 90
 phosphoric acid concentration 56
 Poisson's ratio 110
 Polynomial trial function 97
 Position 2, 11, 12, 27, 29, 110
 atomic 110
 Pressure 31, 51, 65, 67, 76, 109, 110
 gas 109
 Problem 15, 16, 21, 27, 28, 54, 55, 56, 72, 73,
 74, 75, 78
 balance 21
 critical heat transfer 56
 elasto-plasticity 16
 fluid-dynamic 27
 heat exchanger fouling 56
 thermal 54

Properties 3, 4, 11, 63, 64, 67, 95, 96, 106,
107, 108
elastic 107, 108
thermophysical 3, 4, 11, 108
Protective coatings 107
Pseudoplastic fluid obeying 75

R

Refractory interstitial nitride 64
Renewable energy sources 44
Residual 64, 109, 110, 113
oxides 109
stresses 64, 110, 113
Resistance 55, 64, 107
oxidation 64
thermal 55
Reynolds effect 6
Rheological law 76
Richardson number 13

S

Scanning electron microscopy 66
Scavenging process 45
Siegel's approach 74
Simple 5, 76
algorithm 5
cylindrical duct 76
Simulate hydraulic phenomena 27
Simulation(s) 46, 107
engine inlet system CFD 46
techniques 107
Ski jump spillways 27, 28
Smoothed particle hydrodynamics 26
Solar 89, 90, 91, 92, 93, 94, 95, 98, 101, 103,
104
desalination system 90, 91
detector 94
distillation system 89
distiller prototype 93
heater 89, 90, 95, 98
oscillations 98, 101
water 94, 101
Solar energy 89, 90, 92
heaters 89
Solar irradiation 102
intensity 102
Solar radiation 93, 97, 98, 99, 100, 101, 104

intensity 97, 100
Solid works flow simulation (SWFS) 46
Sputtering 65, 66
process 65
techniques 66
Stresses 31, 65, 107
deviatoric 31
intrinsic 65
mechanical 107
Stroke 45
System 1, 45, 74, 75, 89, 90, 91, 93, 94, 100,
103, 104
algebraic 89
cooling 1

T

Tensor 18, 51
second Piola-Kirchhoff stress 18
viscous shear stress 51
Thermal 1, 4, 13, 51, 64, 73, 78, 94, 107
balances 94
behaviour 1
conductivity 4, 13, 64, 78, 107
development 73
enthalpy 51
expansion coefficient 4, 13
Thermo-convective transfer 74
Turbulence kinetic energy (TKE) 44, 49

V

Vector function 16

W

Waste heat recovery 56
Water 26, 31, 32, 33, 35, 36, 39, 41, 89, 90,
91, 92, 93, 94, 98, 100, 101
condensed 93
drinking 26
heater 90
thick swab-rich 89

X

X-ray diffraction analysis 67
XRD diffraction 64



Zied Driss

Prof. Zied Driss is a full-time Professor in the Department of Mechanical Engineering at the National School of Engineers of Sfax (ENIS). He received his Engineering Diploma in 2001, his Master Degree in 2003, his Ph.D. in 2008, and his HDR in 2013 in Mechanical Engineering from ENIS at the University of Sfax, Tunisia.

He is interested in developing numerical and experimental techniques for solving problems in mechanical engineering and energy applications. Also, his research has been focused on the interaction between Computational Fluid Dynamics (CFD) and Computational Structure Dynamics (CSD) codes. As a result of his research, he is the principal or co-principal investigator on more than 250 papers in peer-reviewed journals, more than 500 communications to international conferences, 30 books, and 80 books chapters. Also, he is the main inventor of 12 patents. Currently, Prof. Driss is a Team Leader in the Laboratory of Electromechanical Systems (LASEM), an Editorial Board Member and reviewer for different international journals, an Editor for different books, a General Chair of two bi-annual international conferences, and an active member in different national and international associations.